Universiteit Utrecht

Opleiding Natuur- en Sterrenkunde

Modeling the extraction of tidal energy from the hypothetical Orkney Islands Dam (northern North Sea) and from turbines in a tidal inlet

Bachelor Thesis

Christian Lemmens

Supervisors:

Prof. Dr. Huib de Swart
IMAU

Dr. Erik van Sebille
IMAU

MSc Tjebbe Hepkema
IMAU

July 15, 2017

Abstract

This thesis contains two numerical analyses for two different models that simulate tidal motions. The first is a fundamental model describing a tidal inlet connected to the open sea by a 2 kilometers channel. The research focuses on the speeds through the channel, the water level in the inlet and eventually the power that can be obtained when adding a higher, speed dependent, value to the bottom drag already present. After a couple of iterations this results in a maximum power of 94.34 MW. As an extension the channel is split into one open and one turbine channel and it is found that on basins of sizes beneath 100 km^2 the open channel has a negative effect on the maximum obtainable power from the turbine channel and on basins of sizes above 1000 km^2 the open channel has no influence on the maximum obtainable power. The second is a full blown numerical model of the northern North Sea, mapping the water levels and velocities of the water through the Orkney channel. A dam is connected to the mainland and an open grid point with high bottom drag to calculate the power obtainable over this area. The power available in this model has an average of 3.71 GW, adding up to an energy supply of 32.5 TWh/yr. This hypothetical dam changes the tidal motions around the dam as well as along the United Kingdom's east coast, which could be of influence on the sea and plant life in these areas.

Contents

1 Introduction

It is widely believed that, in order to decrease the CO2 emissions below risky levels without having to reduce in energy use, the world needs more renewable energy. There are already many ways of doing so, like solar energy and wind energy. Another strategy, that is generally less known, is to extract energy from the tidal currents and from the difference in tide induced water levels. In contrast to solar energy and wind energy, which are dependent on weather conditions, tidal energy is permanently available. According to Soerensen and Weinstein (2008) the usable global amount of tidal energy is around 800 TWh yr^{-1}. This might seem a fraction of the global human energy demand, 19771 TWh yr^{-1}. However, for countries on the coasts with high tides, like the United Kingdom, this part is far more significant. The estimated extractable energy from tides in the UK is 50 TWh yr^{-1} (Yates et al., 2013). This is 14.5% of the total energy use of 345 TWh yr^{-1}(2013).

There are three main methods of extracting energy from the tides (Rourke et al., 2010). A tidal barrage builds up potential energy by creating a difference in water level of a basin and the open sea. A dam like in figure 1 is built across a bay or estuary, embedded with turbines. Some tidal barrages only use ebb or flood generation, while others use two-way generation. Two-way generation reduces the period of non-generation and lowers the peak power output, making cheaper turbines capable of doing the job. When high tide is building up in the open sea, the pressure difference pushes water through the turbines filling the basin. Eventually, when high tide is reached, the water level will start reducing to below the basin water level creating a reverse pressure difference and thus a reverse water flow. In addition, sluice gates are often present to build up potential energy in a more effective way. This method works best at coasts with high tidal ranges, because the potential energy of the water will be greater. The La Rance tidal barrage is a power plant that extracts potential energy from the 10 meter high tidal range present. This tidal inlet in northern France has proven its effectiveness since its completion in 1966. The average generated power is 240 MW, adding up to 480 GWh per year and that makes it the largest energy supplier of its kind at the moment. Unfortunately, construction of this method implies high costs and potential environmental risks for the basin and nearby sea. The House of Parliament: Parliamentary office of Science and Technology (2013) investigated the environmental impact of tidal barrages. The turbines and changes in sediment transport and water quality could have a negative impact on ecology. However, these risks are highly dependent on the geological location and hard to determine in advance. Another method is tidal stream generation, which is best comparable with the method of extracting energy from wind currents with wind turbines. This is the most affordable and environmentally friendly method. As seen in figure 2 and described by Rourke et al. (2010) devices can be placed individually to extract the kinetic energy during both the ebb and flood period. At the European Marine Energy Center several turbine types are tested at full-scale. The two most effective operational projects are the Ramsey Sound project and the SeaGen Strangford Lough project, both delivering 1.2 MW (EMEC, 2017). Besides the kinetic and potential method, there is a third method, described by Hulsbergen et al. (2008) combining the two: Dynamic Tidal Power. Unlike the tidal barrage, where a dam is placed along the coastal line, a dam is placed perpendicular out of the coast so that it does not only obstruct the tidal water elevation, but also the tidal current. A hypothetical dam and its influence on

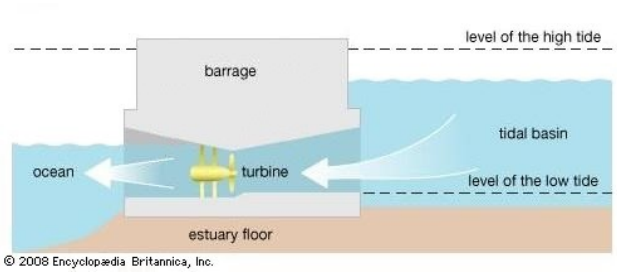

Figure 1: Sketch of the working of a tidal barrage. The barrage partly blocks the water from from flowing, forcing it to flow through the turbines due to the height difference on both sides of the barrage.

the water levels on both sides is shown in figure 3. This results in a pressure difference over the dam and thus a potential energy available to let through the dam. This phenomenon was first described in 1996 by Kees Hulsbergen & Rob Steijn. Several analyses has been done on placing such a dam. Hulsbergen et al. (2008) computed a dam configuration in China and Young Hyun Park (2016) computed one on the west coast of Korea. No DTP dam has been build so far, but plans to apply this method in China and Korea are being studied by Hulsbergen et al. (2008).

1.1 Simple model for extracting energy from a tidal inlet

The first approach is a fundamental model of a tidal inlet by the coast. A large inland basin is connected with the open sea by a channel. The tidal elevation of the sea causes a flow through the channel causing tidal elevations in the basin. This principal is sketched in figure 4. The flow of water is directly dependent on a difference in water level of the basin and the ocean. A tidal inlet describes one or more channels that connect an inland lagoon to the open sea. Neat examples of lagoons connected by a channel are the Broad Water lagoon in Wales and Lake Lllawarra in Australia. Also, at the Cardiff lagoon, the UK government is working on a plan for harvesting energy from the high tidal amplitudes at stake. An oscillating water current will occur in the channel with a period equal to that of the tidal water level at the open sea. Subsequently an oscillating tidal water level will occur in the lagoon. The split tidal inlet, introduced by Cummins (2013), consists of two channels. Of these channels one is open, and the other is embedded with a turbine fence distributed over the cross section homogeneously. Cummins used an analytical model of the inlet by comparing it to an electric circuit. Proposing one simple example Cummins shows the ideal basin area with fixed initial conditions for a split tidal inlet. The dependency on the drag coefficient has not been studied by Cummins. Therefore this study will quantify the dependency of the generated power on the drag force by the turbines as well as the dependency on the basin area. The numerically found ideal basin area will be compared with the ones found by Cummins. This will be done for the single channel inlet and the split channel inlet.

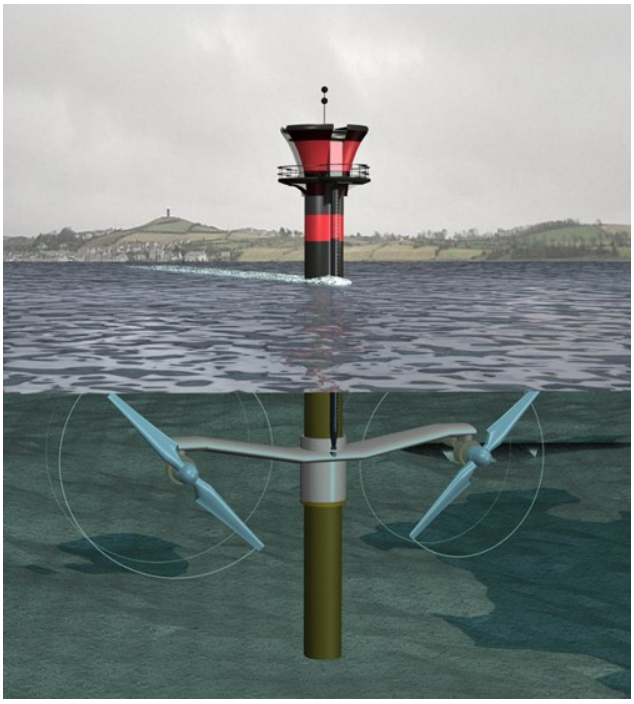

Figure 2: A tidal stream generation device. This device extracts kinetic energy from the tidal currents just like a wind turbine does from the wind current.

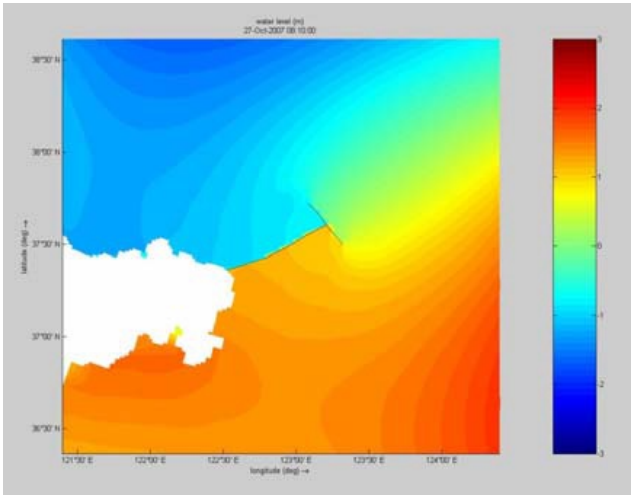

Figure 3: Visualization of the water level distribution around a DTP dam. The Dam blocks the tidal current that originally moved along the coast. Blue is relatively low water and red relatively high water.

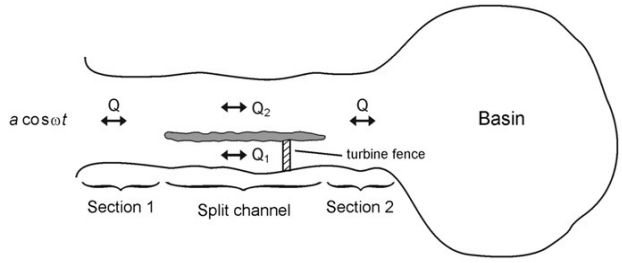

Figure 4: Sketch of a split tidal inlet as described by Cummins (2013). Q_1 and Q_2 denote the fluxes through the channels, where the total incoming flux should equal the total out-coming flux. One channel is open with bottom drag coefficient c_d adopted from Cummins (2013) and the other is embedded with a turbine fence creating a total drag coefficient $c_t + c_d$.

1.2 A full blown numerical model to study tidal power from the Orkney Islands dam

The Orkney Islands form an island group just north of the mainland of Scotland. The area is known for the high speed tidal currents that occur between the island group and the mainland, and between the northern and southern part of the islands. These high tidal velocities are needed to be a good host for a dynamic tidal power plant. In addition, the Orkney Islands are located in such a way that they almost form a block for the tidal current going around northern Scotland. When placed correctly, only a few hypothetical dams could form a full block of the tidal current, forcing it to go around the islands with almost no distortion. It is this characteristic that make the Orkney Islands a very promising host. As explained in A.1.2 the maximum power output of the power plant is proportional to the length of the dam by $P \propto D^{5/2}$. Unfortunately the costs of construction also increase exponentially with longer dam lengths. The Orkney Islands can be used as a geological extension of the artificial dam by around 70 km(figure 5), increasing the potential power output but remaining the costs of construction for only the artificial dam.

Previous research on several hypothetical dams has been done by Hulsbergen et al. (2008). As can be read in A.1 the numerically found water levels and currents were used to analytically determine how much power the dams would deliver. This analytical approach is a good start but does not take into account the geology around the dam, which may affect the influence of a semi-closed dam. Therefore, in this research the power will be numerically found for each time step using a full blown numerical model in Delft3D.

1.3

Overall, in this thesis a close look will be given at these two different ways of extracting energy from the tides by the use of numerical models. First the theory behind the tides in general will be explained in section 2, followed by a specified theory per model. Thereafter, the results of the tidal inlet model will be thoroughly examined in section 3 and the results of the hypothetical Orkney Dam in section 4. The results of both models will discussed in

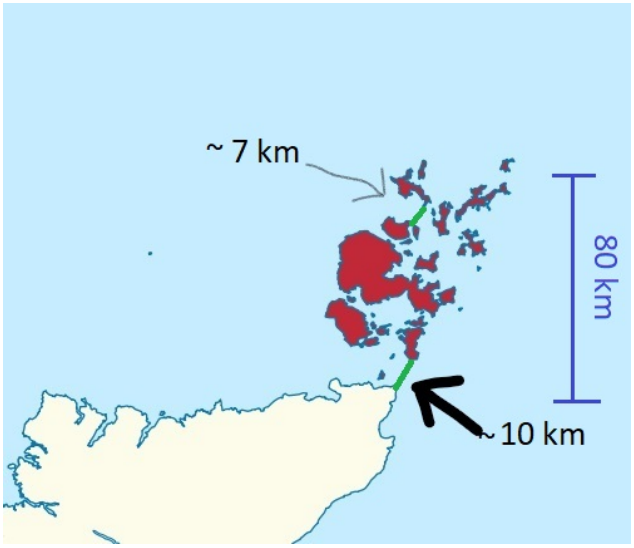

Figure 5: The Orkney Islands above Scotland. The Thick arrow shows the location of the hypothetical dam, partly filled with turbines, and the thin arrow shows the extra hypothetical dam to force the tidal wave around the upper islands by an extra 70 kilometers.

section 5. Finally, a conclusion and an outlook for further research on the models will be given.

2 Theory

2.1 Background on tides

The tidal motions in the world's oceans are a result of the changing relative gravitational forces of the Earth, moon and sun. To begin, one should understand the two body system of gravitational spherical objects, so lets start with the moon and earth in a two dimensional side view. The gravitational forces between the moon and earth causes a orbit around the center of mass for both bodies. This orbit causes a homogeneously centrifugal force on the entire earth opposite to the moon and equal in magnitude to the gravitational force of the moon on the center of mass of the earth (equation 1).

$$F_c = \frac{2GM_{moon}M_{earth}}{r^2}, \tag{1}$$

where G is the gravitational constant, M_{moon} the mass of the moon, M_{earth} the mass of the earth and r the distance from the earth's center to the center of mass of the two body system. In addition, the moon attracts all points on earth to the moon's center. These forces however are not homogeneous because they are all directed at one point with magnitude

$$F_g = \frac{2GM_{moon}M_{earth}}{(r-a)^2} \tag{2}$$

where a is the distance from the earth's center. This results in a net force called the tide-producing force (Butterworth and Heinemann, 1999) and has a size proportional to $\frac{1}{r^3}$ as

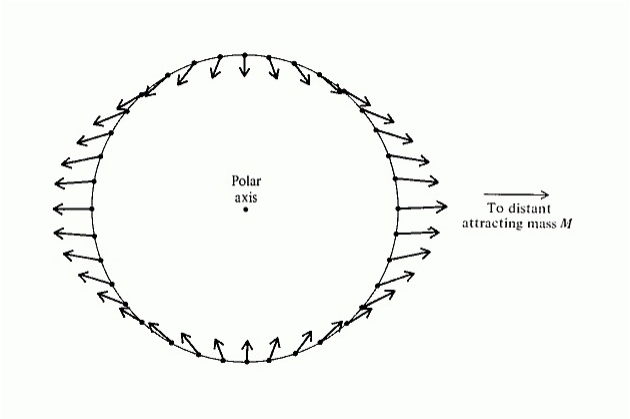

Figure 6: Tidal forces relative to the Earth's center due to a distant attracting mass.

shown in equation 3.

$$F_t = \frac{2GMma}{r^3} \tag{3}$$

The tidal force at the points with their zenith directing perpendicular on the moon are directing to the earth's center, while the points with their zenith parallel to the moon are directing away from the earth's center. So the water surface is squeezed in the directions as shown in figure 6 delivering two high tide and two low tide areas. Also, from equation 3 can be explained why the tidal contribution of the moon is larger than that of the sun by a factor 2.5. Although the sun is much heavier, the closer distance of the moon plays a much bigger role due to the cubed proportionality. So it is clear now that tidal forces are caused by the gravitational forces of the moon and sun, but how do the oceans react to these forces?

The earth turns around its own axis, giving a fixed point the experience as if the sun and moon have orbited around the earth. Naturally this is not the case, however the effect is the same, resulting in a sinusoidal behavior of the angle and size of the gravitational forces. This tidal phenomenon is called the semi-diurnal tide, shortly noted as the M2-tide. When the moon seems to have orbited a quarter further, the same points become low tide points (see figure 6). Since the earth turns a full 360 degrees every day two tidal high tides should occur. However, the moon itself is also in an orbit around the earth in the same direction as earth's rotation. Therefore the the M2-tidal period is 12 hours and 25 minutes, slightly longer than the half day S2-tidal period. Other effects worth mentioning are the diurnal tide which becomes stronger on greater latitudes, the declination of the moon and the relative positions of the moon and sun with respect to the earth. The last is responsible for spring and neap tides. Spring tides occur when the moon and sun are aligned, enforcing each other. Neap tides occur when they are in a right angle, canceling each others effect. Water tends to move to the two points on earth that are in line with with the earth moon alignment. Since these points oscillate, water will flow in a mixed semi-diurnal pattern along the coasts. These are the tidal currents that are interesting to investigate, because they are mostly close to population and thus suitable for power generation.

2.2 Model of Tidal Inlet

2.2.1 Bases of the model

The model used in this research is built up from one representing a single open channel connecting the ocean to a lagoon. The M2 tidal amplitude is 1 meter with a period of $T =$ 12 hours and 25 minutes, the channel is 2 km long, 1 km wide and 10 meters deep. The flow rate trough the channel and the rise and fall of the water level in the lagoon are then related by

$$\frac{du}{dt} = -g\frac{\zeta - \zeta_0}{L} - \frac{c_d|u|u}{h} \tag{4}$$

$$S_b\frac{d\zeta}{dt} = uA \tag{5}$$

where, u is the speed of the water in the channel, L is the channel length, A the channel cross section, S_b the basin surface area, ζ the basin water level, $\zeta_0 = Zcos(\omega t)$ the ocean water level, $\omega = \frac{2\pi}{T}$, g the gravitational acceleration, c_d the typical bottom drag coefficient and h the depth of the channel. Explicitly given, the acceleration of the water in the channel is driven by the water level difference on both sides of the channel. The third term in equation 4 is a friction term that acts over the whole length of the channel. For an open channel this term consists only of the bottom drag, quantified by its drag coefficient c_d and working over the whole bottom area of the channel. Equation 5 describes the equality between the change in volume per time unit of the basin and the volume transport through the channel. The rise and fall of the water level of the basin is in turn dependent on the speed through the channel. This model applies only when the length of the channel and the sides of the lagoon are much smaller than the M2 tidal wavelength and the water level difference is much smaller than the depth of the channel and the lagoon.

2.2.2 Adding turbines for energy extraction

In addition, the drag term must be extended in order to extract energy from the flow trough the channel. Now, to do calculations for the turbine channel it is very important to understand that at the channel the mass inflow must equal the mass outflow, because otherwise matter would disappear or add without reason. This principle is called the conservation of mass and implies that the flow speed in a channel is independent on the position in the channel, regardless the location of the fence. Therefore, the drag coefficient of the turbine channel can be handled just the same as the bottom drag coefficient, namely over the whole bottom area. This is of great importance because now it is possible to just take a higher drag coefficient in the turbine channel to calculate the speeds and water levels. Therefore, a turbine drag coefficient is added to the bottom drag coefficient, resulting in a total drag coefficient of $c_{tot} = c_d + c_t$. The turbine drag however works different on the water than the bottom drag. The bottom drag term from equation 4 is quadratic with the speed while a turbine drag term is linear with the speed. So $c_t = \frac{\hat{c}}{|u|} \propto \frac{1}{|u|}$. Thus equation 4 is replaced by equation 6. The water level change is still calculated by equation 5.

$$\frac{du}{dt} = -g\frac{\zeta - \zeta_0}{L} - \frac{(c_d + c_t)|u|u}{h} \tag{6}$$

These turbines deliver a power output defined by

$$P = \rho S c_t |u| u^2 = \rho S \hat{c} u^2, \tag{7}$$

where S is the bottom area of the channel. In order to find the maximum power output the model will be run for different turbine drag coefficients defined by the drag constant $\hat{c}$. By taking the average power from each separate run, the dependency from the power on the drag constant can be visualized. This will show that there is a maximum power for a single drag constant. All lower drag constants extract to little from the kinetic energy of the flow. All higher drag constants reduces the flow such that too little water volume exchanges between the channel and the open sea.

2.2.3 Split tidal channel inlet

The models from section 2.2.1 and 2.2.2 can now be combined to create a split tidal channel inlet. A cross sectional view is sketched in figure 7. The speeds in the different channels follow by equations 4 with $u \to u_1$ and 6 with $u \to u_2$. The water level of the lagoon follows by the total of the fluxes trough the channels.

$$S_b \frac{d\zeta}{dt} = u_1 A_1 + u_2 A_2, \tag{8}$$

where u_1 is the flow speed trough channel 1, u_2 is the flow speed trough channel 2, A_1 is the area of channel 1 and A_2 is the area of channel 2. The power is calculated by equation 7 with $u \to u_2$.

2.2.4 Numerical Runge-Kutta Model

A straight coast is interrupted by a 1 kilometer wide and 10 meters deep channel, resulting in a cross sectional area of $A = 10^4$ m^2. This channel has a straight constant rectangular shape until reaching the lagoon after 2 kilometers. The depth of the lagoon has no effect as long as it is lower than the channel. Furthermore, the tidal elevations ζ_0 of the open sea have an amplitude of 1 meter and a period of 12 hours and 25 minutes. To obtain data from this idealized model the "classical Runge-Kutta method" is applied as explained by Butcher (2007). This method is best to solve polynomial differential equations like equation 4, 6 and 8 because it gives the exact solution of a fourth degree polynomial (or less), where the max degree in these differential equations is 3. In short, for a function $y' = f(t, y)$ each time step Δt a new y is calculated as follows.

$$y_{i+1} = y_i + \frac{\Delta t}{6}[k_1 + 2k_2 + 2k_3 + k_4] \tag{9}$$

where,

$$k_1 = f(y_i, t_i)$$
$$k_2 = f(y_i + \frac{\Delta t}{2} k_1, t_i + \frac{\Delta t}{2})$$
$$k_3 = f(y_i + \frac{\Delta t}{2} k_2, t_i + \frac{\Delta t}{2})$$

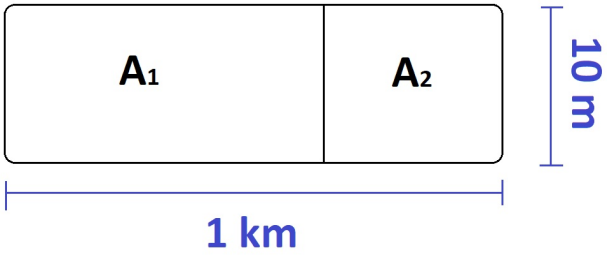

Figure 7: Sketch of the cross section of a split channel tidal inlet. Channel 1 is open and has a bottom drag coefficient of $c_d = 0.0025$ and channel 2 is implemented with a turbine fence having a speed dependent drag coefficient.

$$k_4 = f(y_i + \Delta t k_3, t_i + \Delta t)$$

For each time step this Runge-Kutta method is able to calculate the speeds and water level when given the conditions from the previous time step. The model and Runge-Kutta method are put in a python script that calculates at every time step Δt automatically until the preferable end time. Having the speed u_2 through the turbine channel with a fixed drag constant $\hat{c}$ for every time step , it is now possible to find the power for every time step as well by equation 7. Giving some time for the system to become stable a set of 20 M2 tidal periodsa are chosen to take an average over all time steps of all the calculated powers. Now it is possible to obtain the average power from the turbine fence for a certain drag constant.

To research which initial conditions are best, the complete set of calculations will be repeated over changing initial conditions, storing the average power for each initial condition. In this way the dependency of the power on every term can be plotted, with fixed other conditions. For this research the dependency of the drag constant $\hat{c}$ caused by the turbines and of the basin area S_b are studied. The optimum in these variables will be identified for the single channel tidal inlet as well as a split channel tidal inlet with turbine channel width of 750 meters and an open channel width of 250 meters such that the total width remains 1 km.

2.3 DTP

2.3.1 Delft3D model

For research on dynamic tidal power Delft3D is used for modeling the tidal current on the North West European shelf. Delft3D is one of the world leading modeling software handlers, specialized in investigating hydrodynamics, sediment transport and morphology and water quality for fluvial, estuarine and coastal environments(DEL, 2017). For tidal induced hydrodynamics the FLOW module is ideal to use. This module takes into account all significant present tidal effects caused by the sun and moon. In explicit these are the semi-diurnal(M2, S2, K2, N2), diurnal(K1, Q1, P1, O1) and long period(MF, MM, SSA) tidal modes. At the

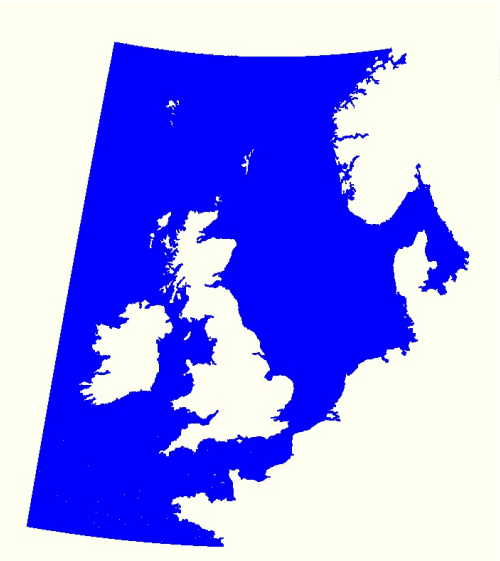

Figure 8: Simulation area used in Delft3D with boundary conditions at the northern, western and southern boundaries that are connected to the ocean.

open boundaries of the grid the tidal motions due to these components are obtained from already succeeded simulations. These motions are set as boundary conditions and cannot act otherwise during the simulation. For all other grid points the module uses shallow water equations to calculate each time step from the previous one.

$$\frac{\partial u}{\partial t} + u\frac{\partial u}{\partial x} + v\frac{\partial u}{\partial y} - fv + g\frac{\partial \eta}{\partial x} = 0 \tag{10}$$

$$\frac{\partial v}{\partial t} + u\frac{\partial v}{\partial y} + v\frac{\partial v}{\partial x} + fu + g\frac{\partial \eta}{\partial x} = 0 \tag{11}$$

$$\frac{\partial \eta}{\partial t} + \frac{\partial (\eta + h)u}{\partial x} + \frac{\partial (\eta + h)v}{\partial y} = 0 \tag{12}$$

with u and v the spatial velocities, f the Coriolis force, g the gravitational constant, η the water elevation and h the water depth. Physical parameters, such as the gravitational constant g, the horizontal eddy viscosity and the water density ρ are hold on standard values.

This simulation uses a grid frame that is spherical and has 682 x 626 grid points with a constant latitude grid spacing of 2.77 km. The longitude grid spacing is different because longitude lines get denser as the latitude increases on a spherical coordinate system. Important is the longitude grid spacing at Orkney which is around 2.3 km, having grid areas of 6,37 km^2. Altogether the model spans the area printed on figure 8. For a more global relative inside, this is longitude 12W - 15E and latitude 47N - 64N. A timescale of two M2-tidal periods is chosen to calculate the velocities and water levels throughout the grid frame for every time step of 5 minutes. Also, in Delft3D fundamental changes can be done to the domain, like adding dams, wind and changing the bottom roughness.

2.3.2 Method

At first results will be obtained for the undisturbed situation at the North West European shelf. To test the simulation a contour plot of the tidal phases will be compared with known data. Preliminary, there will be zoomed in on the Orkney Islands to visualize the tidal motions that are present. In explicit, overall water levels and speeds as well as the M2 amplitudes and phases will be examined to understand how energy can be extracted. Second the Delft3D model will be modified such that a dam with an open space is created. Several open dam configurations will be simulated to find which one results in the highest speed through the open space. Ultimately the best dam configuration is upgraded as if it has turbines, by giving the open space a specified bottom drag, suited to a certain flux reduction. The determination of this bottom drag is explained as follows.

For this model it is chosen to reduce the speed through the open space by about $\frac{2}{3}^{rd}$. Unfortunately it is uncertain how much bottom drag is needed to cause this reduction. To find this an iteration process has to be done. A wild guess of the input bottom drag coefficient c_{d3d} needed is made resulting in a certain amplitude u_0. If the resulting amplitude is less than the desired amplitude the bottom drag should be chosen lower and vice versa. After a couple of times a bottom drag causing the desired amplitude will be found. Next, a second issue arises. Just like with the tidal inlet the bottom drag is defined as constant over different speeds, whereas the turbine drag coefficient is proportional to $\frac{1}{|u|}$. In order to find the same average power an adjustment must be made for the bottom drag coefficient.

$$\hat{c} = c_{d3d}\frac{8|u_0|}{3\pi} \tag{13}$$

The power is now calculated for each time step, just like with the tidal inlet by equation 14, only different in calculating $\hat{c}$ from c_d due to the speed independent bottom drag during the simulation. The bottom area where the drag works is equal to the grid area of 6.37 km^2.

$$P = S_g\rho\hat{c}u^2 \tag{14}$$

After this last simulation the speeds over the turbine area and the water levels around the dam will be examined. With the speeds the power will be calculated over each time step and averaged over the time scale. In addition the influence of the dam and turbines on the area will be shown by looking at the head over the dam and the changes in tidal motions of the area.

3 Results of the numerical model of a Tidal Inlet

3.1 Single Channel Inlet

Figure 9 shows the average power versus the turbine drag constant $\hat{c}$ from a single channel inlet with a basin area of $S_b = 100$ km^2. The expected optimum of extracting enough energy and letting through enough flux to be returned later is thus true. For this case the maximum obtainable power outcome is when $\hat{c} = 0.0347$ m/s delivering $P = 35.56\ MW$. Figure 10 shows the average power versus the basin area S_b for $\hat{c} = 0.0347$ m/s. The optimum is found

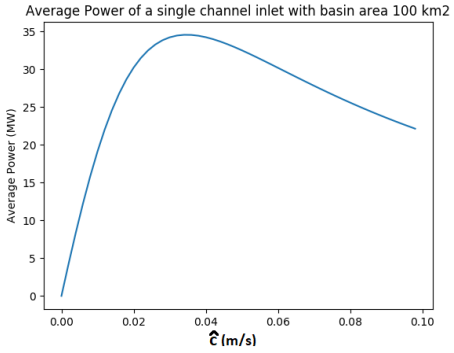

Figure 9: Average power versus turbine drag constant $\hat{c}$ of a single channel inlet with basin area $S_b = 100$ km^2.

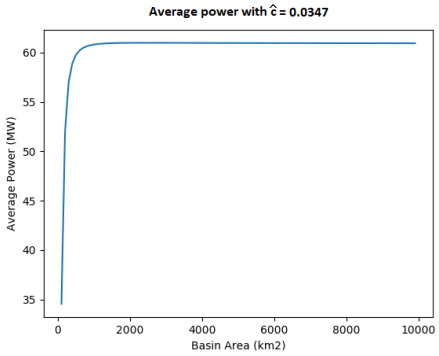

Figure 10: Average power versus basin area S_b of a single channel inlet with turbine drag constant $\hat{c} = 0.0347$ m/s

to be at $S_b = 2500$ km^2 with $P = 61$ MW. Since this is optimum area is significantly higher than the area used in the first iteration step a second iteration has been done. Figure 11 shows the average power versus turbine constant for a basin area of $S_b = 2500$ km^2 it. It shows the same behavior as the first iteration but shifted to the left, with maximum drag constant of $\hat{c} = 0.0117$ m/s resulting in an average power of $P = 94.34\ MW$. At last figure 12 shows that the ideal basin area of $S_b = 2350$ km^2 does not differ much from the previously found and $P = 94.47\ MW$. Therefore these can be takena as the ideal values of the basin area S_b and the turbine drag constant $\hat{c} = 0.0117$ m/s. In addition figure 12 shows that the average power barely changes when the basin area gets greater than $S_b = 1000$ km^2. Figure 13 shows that the ideal $\hat{c}$ is the same as with a 2.5 larger basin area in figure 11. Therefore, it can be concluded that all basin areas above 1000 km^2 result in the same order of magnitude in power generation.

3.2 Split Channel Inlet

For the split tidal inlet the same iteration process has been done. The turbine channel now is 750 meters wide and the open channel 250 meters, remaining the total width of 1 km. Figure 14 shows the average power versus the drag constant $\hat{c}$ with basin area $S_b = 100$ km^2. The

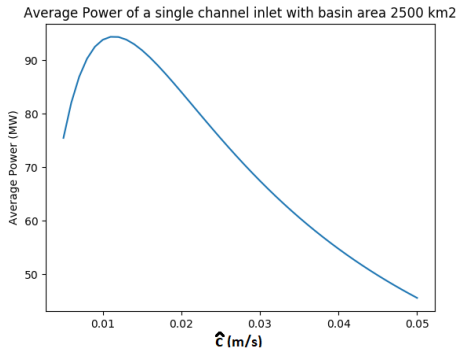

Figure 11: Average Power versus $\hat{c}$ of a single channel inletwith basin Area $S_b = 2500$ km^2

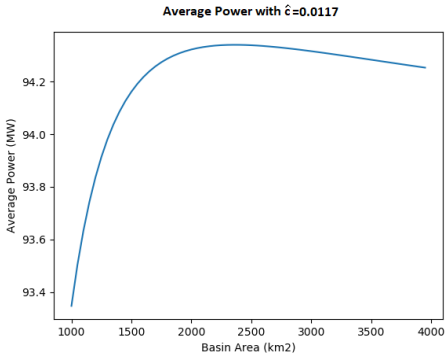

Figure 12: Average power versus basin area S_b of a single channel inlet turbine drag constant $\hat{c} = 0.0117$ m/s

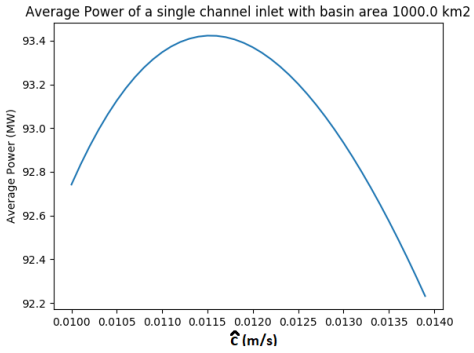

Figure 13: Average power versus turbine drag constant $\hat{c}$ of a single channel inlet with basin area $S_b = 1000$ km^2.

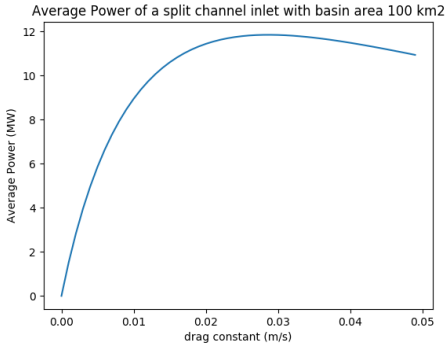

Figure 14: Average power versus turbine drag constant $\hat{c}$ of a split channel inlet with $S_b = 100\ km^2$

optimum reaches $P = 11.85$ MW when $\hat{c} = 0.029$ m/s. This value of $\hat{c}$ is taken to finish the first iteration in figure 15 showing the power versus the basin area S_b reaching its maximum of $P = 52.25$ MW when $S_b = 1500$ km^2. Again a conclusion can be made that the power barely varies when the basin area gets greater than 500 km^2. Just as in section 3.1 a new iteration is needed because of the great difference in power as well as in basin area before and after the first iteration. So the optimum basin area of figure 15 has been taken for this new iteration. Figure 16 shows the average power versus the drag constant $\hat{c}$ with basin area $S_b = 1500$ km^2. The optimal drag constant for this setup delivers an average power of $P =$ 71.06 MW with $\hat{c}$ 0.0117 m/s, just like the optimal drag constant for the single channel inlet with the same order of magnitude in basin area. To complete this iteration this optimum is taken on varying basin areas. Figure 17 shows the average power versus basin area S_b with drag constant $\hat{c} = 0.0117$ m/s. The optimal basin area is found at $S_b = 2000$ km^2. Hence, the optimal setup for a split tidal channel with a channel ratio of 750:250 has a basin area of S_b = 2000 km^2 and a turbine fence with drag coefficient $c_t = \frac{0.0117}{|u|}$. This results in a maximum power output of $P = 71.13$ MW. In addition figure 18 shows the optimal drag constant $\hat{c}$ with basin area $S_b = 1000$ km^2. Again this remains the same as for greater basin areas with $\hat{c} = 0.0117$ m/s resulting in a power of $P = 70.43$ MW.

Furthermore, figure 19 shows the average power versus turbine channel width for a basin area of $S_b = 100$ km^2 and a turbine drag constant of $\hat{c} = 0.0347$ m/s. It is clearly visible that the power grows exponentially when enlarging the turbine channel width and reducing the open channel width. Figure 20 shows the same but then for $S_b = 1000$ km^2 and $\hat{c} = 0.0117$ m/s. Here it is clearly visible that the power grows linearly when enlarging the turbine width and reducing the open channel width.

4 Results of the hypothetical Orkney Dam

4.1 The current situation without hypothetical dam and turbines

To begin the current situation is plotted as calculated by Delft3D. Figure 21 shows the M2 tidal phases of the north west European shelf. The few points where all phase lines converge

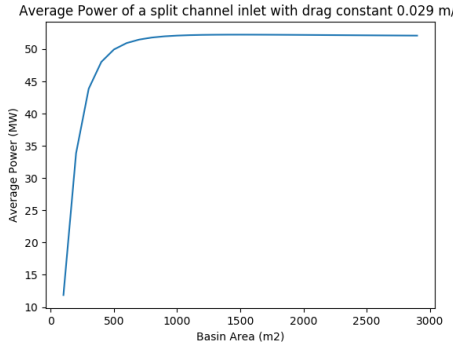

Figure 15: Average power versus basin area S_b of a split channel inlet with turbine drag constant $\hat{c} = 0.029$ m/s

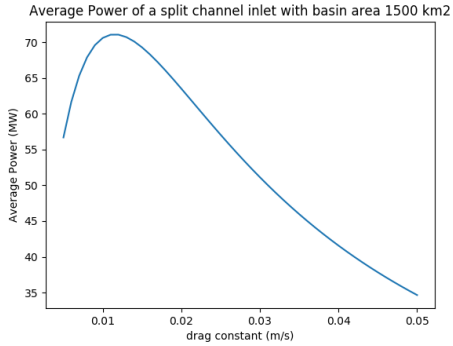

Figure 16: Average power versus turbine drag constant $\hat{c}$ of a split channel inlet with $S_b = 1500\ km^2$

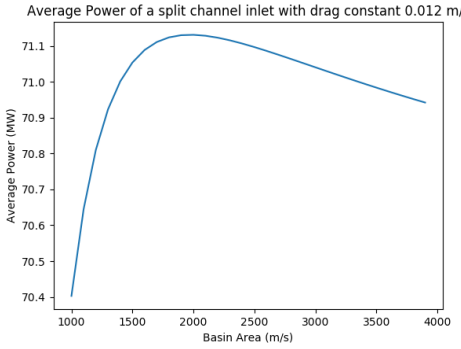

Figure 17: Average power versus basin area S_b of a split channel inlet with turbine drag constant $\hat{c} = 0.0117$ m/s

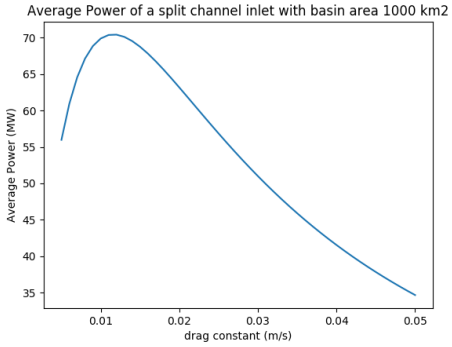

Figure 18: Average power versus turbine drag constant $\hat{c}$ of a split channel inlet with $S_b = 1000\ km^2$

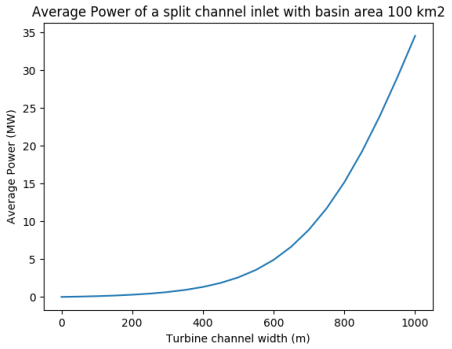

Figure 19: Power versus turbine channel width ($b_1 + b_2 = 1000\ m$ is constant) with $S_b = 100\ km^2$ and $\hat{c} = 0.0347$ m/s.

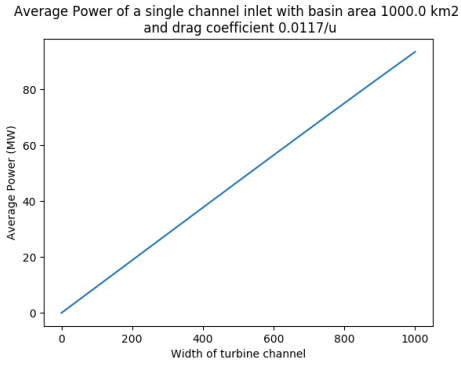

Figure 20: Power versus turbine channel width b2 ($b_1 + b_2 = 1000\ m$ is constant) with $S_b = 1000\ km^2$ and $\hat{c} = 0.0117$ m/s.

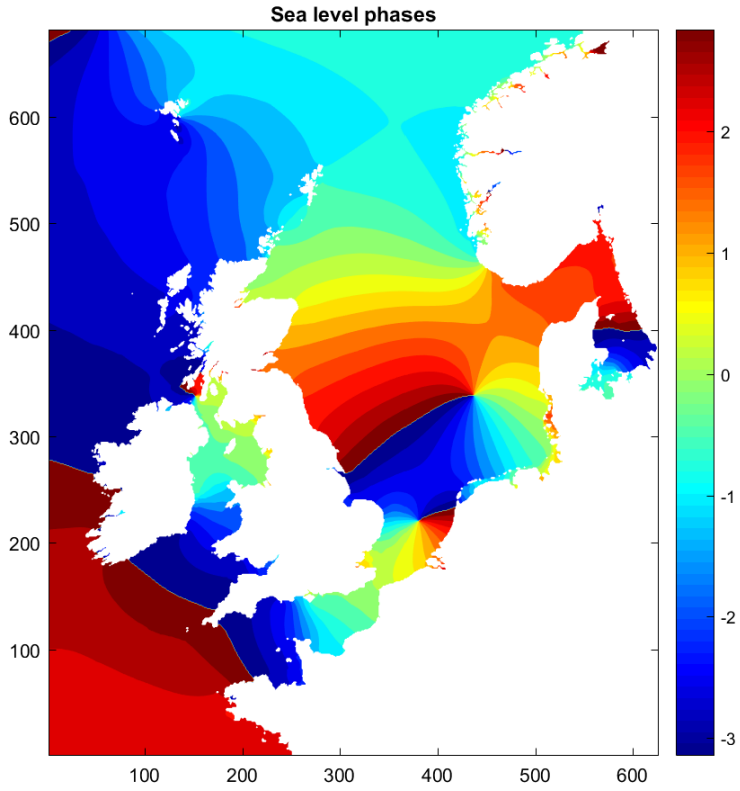

Figure 21: Contour plot of the M2 tidal phases in the seas around the British isles. All areas with the same color have approximately the same phase. Note that dark blue and dark red respectively denotes $-\pi$ and π and thus have a comparable phase.

are called amphidromic points. They are known to have no tidal phase since the tidal wave propagates around these points. One can see the tidal wave propagating around the known amphidromic point in the north sea, north of the Netherlands. Furthermore figure 21 shows that the tidal wave propagates around northern Scotland from west to east to continue its journey along the east coast of the United Kingdom. Figure 22 shows the M2 tidal velocity amplitude (left) and the velocity trough the open space (right) where the turbines will be placed. These high speeds reaching over 3 m/s are ideal for Dynamic Tidal Power. Having an average velocity of 2.36 m/s is a little bit higher than the 2 - 2.20 m/s present tidal velocities at the Pentland Firth as described by Shields et al. (2009).

4.2 A hypothetical dam with turbines at its south west's end

Several dam configurations have been simulated with one clear winner if it comes to magnitude of velocity trough the open space. A Dam having an open space on the southwest delivers the highest speeds trough this open space. Figure 23 shows the velocity trough this south west open space for an open channel space (left) and a turbine embedded space (right). Peak velocities of around 6 m/s are the result of this open configuration. This is almost twice

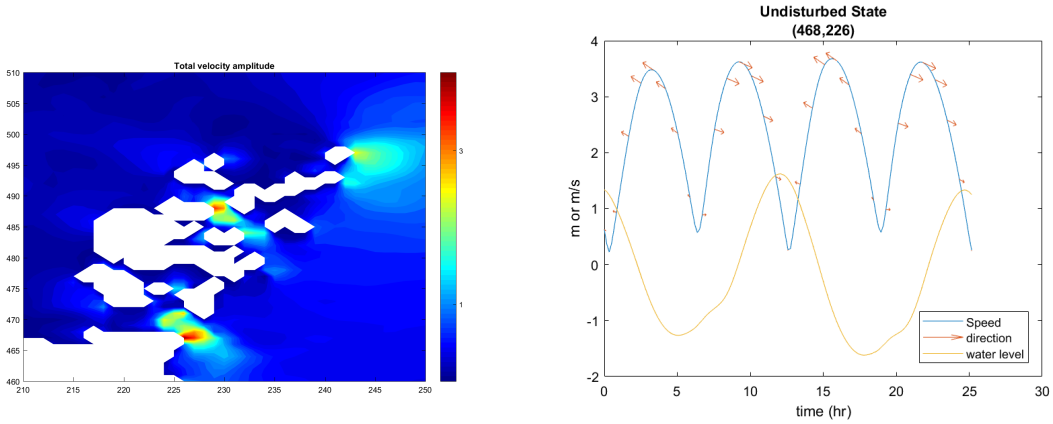

Figure 22: Left: Contourplot of the M2 tidal velocity amplitudes around the Orkney Islands with range 0 - 4 m/s. Right: the water levels and velocities on the virtual location for the turbines.

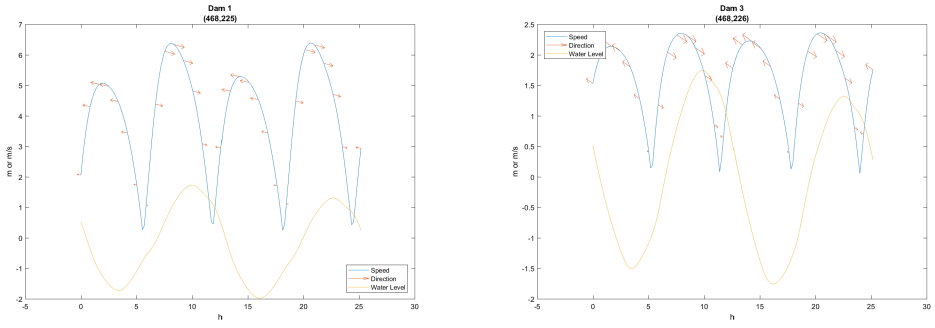

Figure 23: Velocity and water level trough the open space of the dam without turbines (left) and with turbines (right). The M2 tidal period of 12 hours and 25 minutes has passed twice during this simulation

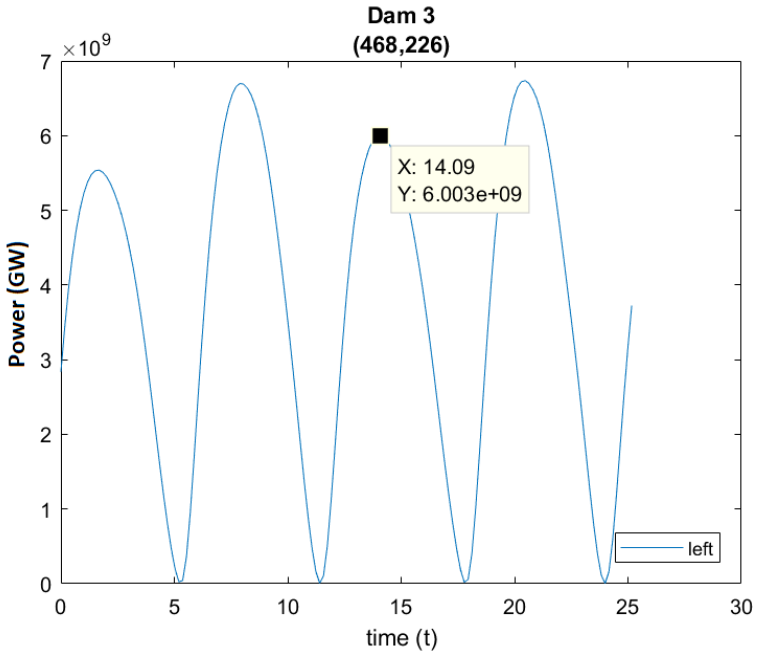

Figure 24: Power of the final dam configuration with $\hat{c} = 0.191$.

as high as the undisturbed velocities trough the channel at Pentlanth Firth. As stated in section 2.3.2 the turbines are represented by a bottom drag such that $\frac{2}{3^t h}$ of the velocity is reduced. The right figure shows with its peak velocity just above 2 m/s that the desired reduction of speed is succeeded. This reduction is caused by drag constant of $\hat{c} = 0.191$ m/s. The power of the dam is now calculated by applying equation 14 to the speeds on every time step. Figure 24 shows the Power output over time for the whole simulation. Also S_2 is the grid area of 6.37 km^2, on which the bottom drag acts and $\rho = 1000$ kg/m^3. The power of this configuration is shown in figure 24 and results in peak powers of around 6 GW and an average power output of 3.71 GW. This would result in an energy supply of 32.5 TWh/yr.

Figure 25 shows the difference in water level between the undisturbed state and the state with the hypothetical dam with turbines. It is visible that the tidal wave moving around England propagates changes its propagation at the dam. Subsequently it also propagates different when leaving the Orkney Islands as can be seen on the east coast of Scotland where the water levels are half a meter higher than normal. Even at the east coast of England a small difference is visible the water level. At all other locations of the north sea no significant changes are shown.

5 Discussion

5.1 Numerical model of a tidal inlet

The numerical model used for this topic is limited several ways. The length, depth and total width of the channels are of influence on the velocities trough the channel and thereby the

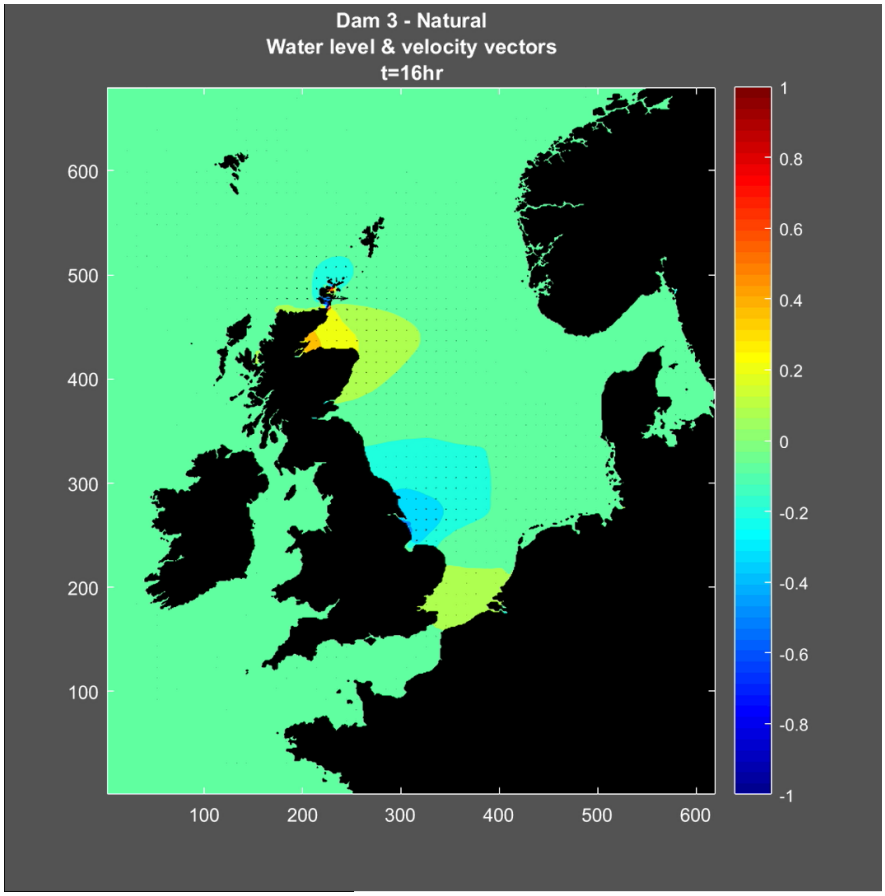

Figure 25: Difference in water level between the undisturbed state and the state with the hypothetical dam with turbines.

power outcome. The velocities in this model are depth averaged, whereas the real velocities trough a channel are distributed differently when applying a bottom drag. It is likely that there are other settings giving higher powers for a basin of these areas. Subsequently the tidal amplitude of the sea has a great influence on the power outcome and is dependable on the geological location of the channel. Furthermore, this model is restricted to channel sizes and basin sizes way smaller than the tidal wavelength present. Otherwise the motions in the channel and basin would not be constant as they are in this model. The tidal wavelength strongly depends on the geological situation, making this model not applicable for every location. Finally, the turbine drag term used in this model works over the whole bottom, while in real it works over the length of the turbine fence. Therefore, when finding the right total turbine drag, the term should be multiplied by factor of $\frac{L}{L_f}$, with L the channel length and L_f the length over which the turbines are distributed.

5.2 The hypothetical Orkney Dam

Given the time available for this research there has not been found a way to locally reduce the grid spacing in order to get more precise results for the area of the hypothetical dam. Doing this will probably deliver more realistic results, since the grid distances are relatively long with respect to the dam size. Also a longer simulation should be done to take along the full spring-neap cycle of the tides. In this model only two M2-tidal periods have been used, making it impossible to know where in the spring-neap cycle the model runs. Furthermore, this model uses an open space where drag is exercised on all the water flowing trough that space, while the water in the two spaces north east of it is completely blocked. Altogether, a more precise model could be made to simulate a more realistic approach of the hypothetical Orkney Dam.

6 Conclusions & Outlook

6.1 Energy extraction from turbines placed in a tidal inlet

Energy extraction from a tidal currents in an inlet has been studied with a simple model. This model is a numerical extension of the analytical model of Cummins (2013). Other than the analytical approach with a bottom stress linear on velocity, this model contains a bottom stress nonlinear on velocity. The 2 km long, 1 km wide and 10 meters high channel inlet at an open sea with a M2 tidal amplitude of 1 m has the following main findings. It has been found for the single channel inlet that the optimum of power generation is reached when the basin area $S_b = 2350$ km^2 and the turbines satisfy a drag constant $\hat{c} = 0.0117$ m/s. An average power output of around 94 MW is reached with this optimum. For the split tidal inlet, where the turbine channel is 750 m and the open channel is 250 m, the optimum is reached when the basin area $S_b = 1500$ km^2 with the same drag constant. An average power output of around 71 MW is reached with this optimum. Also, for both setups it has been found that above a basin area of $S_b = 1000$ km^2 the optimum drag constant is the same with $\hat{c} = 0.0117$ m/s and the power resulting from that grows linear with the turbine channel width. On smaller areas however, as can be seen at a basin area of $S_b = 100$ km^2, the optimum

drag constant is not the same for both setups and the power here reduces exponentially with the turbine channel width. This is enforced by figure 19 and 20. Therefore the exponential dependency is thanks to the contribution of the open channel. It can thus be concluded that for areas below 1000 km^2 the open channel has a negative influence on the maximum extractable energy, while for areas above 1000 km^2 the open channel has no effect. This is explained by the fact that for smaller areas the basin water level will be adapted too fast, resulting in a lower water level difference with the sea. For larger areas this effect goes to zero.

Further research could be done in examining other variables of the split tidal inlet like the total width, length and depth of the channels. Subsequently, the model could be extended such that the flow will temporarily be stopped or even powered, resulting in higher or broader peaks of flow velocity and thus in power.

6.2 Energy extraction from the hypothetical Orkney Dam

A complex Delft3D model has been used to give a numerical insight on the influence of a hypothetical dam located between the Orkney Islands and the mainland of Scotland. A dam was added to the model extended with a turbine grid such that energy can be calculated. By comparing the results of the tidal velocities and water levels of the undisturbed model with that of the extended model the influence of the turbine filled dam has been examined. With the extended model it has been found that a hypothetical dam filled for a 3^{rd} with turbines could deliver an average power of 3.71 GW. This is an energy supply of 32.5 TWh/yr, which is around a 10^{th} of the United Kingdom's energy demand. Of course, this could be a significant contribution in England's clean energy supply. Furthermore the hypothetical dam alters the tidal motions around the dam enormously in current as well in water levels. But even hundreds of kilometers south of the dam along the United Kingdom's east coast a small difference of about half a meter in water level is experienced in time.

Further research on this topic starts adjusting the model such that grid spacing close to the dam is small compared to the size of the dam and such that the geological shapes around the dam are more realistic. The distribution of turbines can be improved by using the whole length of the dam instead of one third. Also, mechanical research on turbines that are best suited for these flow velocities should be done in order to find how much energy will eventually be able to be supplied on the net. For biological purpose, research should be done on the impact on the environment in the Pentlanth Firth channel, due to the significant changes in tidal behavior. Subsequently one should find the impact of the small change in water level along the east coast of the United Kingdom. Sea life as well as plants could be influenced by these changes in a positive as well as a negative way.

7 Acknowledgments

Besides my supervisors, a handful of people should be acknowledged by their contribution to this thesis. First of all inventor of DTP Kees Hulsbergen and Gijs van Banning have given

insight information about the working of this principle and handed out a full blown Delft3D model of the area around England, affecting the tidal happenings on the potential location of the Orkney Dam. Likewise Wei Chen has been of great importance helping out with the MatLab script handling the Delft3D output.

References

2017. *Deltares: about Delft3D*. https://oss.deltares.nl/web/delft3d/about/ [Accessed: May 2017].

Butcher, J.
2007. Runge-Kutta methods. *Scholarpedia*, 2(9):3147. revision #91735.

Butterworth and Heinemann
1999. *Waves, Tides and Shallow Water Processes*. Oxford: The Open University.

Cummins, P. F.
2013. The extractable power from a split tidal channel: An equivalent circuit analysis. *Elsevier, Renewable Energy*, 50(2):395–401.

EMEC
2017. *EMEC: about us*. http://www.emec.org.uk/about-us/ [Accessed: May 2017].

House of Parliament: Parliamentary office of Science and Technology
2013. Environmental impact of tidal energy barrages. (435).

Hulsbergen, K., R. Steijn, G. Banning, G. Klopman, and A. Frohlich
2008. Dynamic Tidal Power - A new approach to exploit tides.

Park, Y. H.
2016. Analysis of characteristics of Dynamic Tidal Power on the west coast of Korea. *Elsevier, Renewable and Sustainable Energy Reviews*, (68):461–474.

Rourke, F. O., F. Boyle, and A. Reynolds
2010. Tidal energy update 2009. *Applied Energy*, 87(2):398 – 409.

Shields, M. A., L. J. Dillon, D. K. Woolf, and A. T. Ford
2009. Strategic priorities for assessing ecological impacts of marine renewable energy devices in the pentland firth (scotland, uk). *Marine Policy*, 33(4):635 – 642.

Soerensen, H. C. and A. Weinstein
2008. Ocean Energy: Position paper for IPCC. (2).

Yates, N., I. Walkington, R. Burrows, and J. Wolf
2013. Appraising the extractable tidal energy resource of the UKs western coastal waters.

A Appendix

A.1 Analytical approach on dynamic tidal power

A.1.1 Head over the dam

Hulsbergen et al. (2008) After the invention of the idea to combine the potential and the kinetic energy of the tides there has been limited research on this subject. Some thought it would not be significantly better than one of the two separate tidal energy resources. However, both analytical and numerical calculations state, that this technique of combining kinetic & potential energy should create a significant head over the dam way. According to the analytical model of Paul Kolkmann the maximum head over the dam equals

$$\Delta h_{max} = \frac{4\pi v_{max} D}{gT}. \tag{15}$$

where D is the dam length and T is the M2 tidal period.

A more realistic approach is the numerical model, which also takes into account effects from the Coriolis force and a realistic sea bed with frictions. For example, in case of the numerical Zunowak model of Rijkswaterstaat (Hulsbergen et al., 2008). This Delft3D model simulates the tidal currents around a Dam in IJmuiden. The model covers the area of the southern North Sea between 51° and 54° latitude with a 1.5 by 1.5 km grid area. Mass conservation, Coriolis force, exchange of horizontal momentum through eddy viscosity and bed friction is taken into account. After investigating straight dam configurations from 20 to 50 km perpendicular on the coast, they found that the numerical head over the dam is around 1.7 times greater than the analytically calculated maximum head for all dam lengths. Needless to say this is the head over a fully watertight dam, so we need a so called effective head Δh_{eff} which also takes into account that water is let through via turbines. So numerically the maximum head of the dam is

$$\Delta h_{max} = 0.05 D V_{max} \tag{16}$$

A.1.2 Power

We now have enough input for an estimation of the maximum generated power from the turbine filled dam, given

$$P_{Elmax} = \rho g \Delta h_{eff} A_t v_t * \eta \tag{17}$$

where A_t is the total flow area of the turbines, v_t the velocity through the turbines and η the efficiency of the turbines. The effective head is linearly dependent on the length of the dam by equation 15. Also $v_t \propto h_{eff}^{1/2}$, so also proportional to $D^{1/2}$ The power also seems to grow linearly from the A_t term as well but this is a misunderstanding. This is because the effective head over the dam becomes smaller if the turbine area grows. It is found that the ideal turbine area takes between 5% & 10% of the total area of the dam. Explicitly given, the turbine area is linear with the dam length.

Given these three proportions to the power of the dam we'll get the following conclusion. The power of the dam is proportional to $D^{5/2}$ and to $V^{3/2}$. Therefore, it's important to scan for locations with high tidal currents and to look for a dam length which is economically efficient to build versus the power generation.